

**HYDROGEN PRODUCTION FROM WATER SPLITTING UNDER VISIBLE
LIGHT IRRADIATION OVER MESOPOROUS-ASSEMBLED $\text{TiO}_2\text{-SiO}_2$,
 $\text{TiO}_2\text{-ZrO}_2$, AND $\text{SrTi}_x\text{Zr}_{1-x}\text{O}_3$ NANOCRYSTAL PHOTOCATALYSTS WITH
BIMETALLIC Pt-Ag LOADING**



Nicharee Chaona

A Thesis Submitted in Partial Fulfilment of the Requirements
for the Degree of Master of Science
The Petroleum and Petrochemical College, Chulalongkorn University
in Academic Partnership with
The University of Michigan, The University of Oklahoma,
Case Western Reserve University and Institut Français du Pétrole
2012

Thesis Title: Hydrogen Production from Water Splitting under Visible Light Irradiation over Mesoporous-Assembled $\text{TiO}_2\text{-SiO}_2$, $\text{TiO}_2\text{-ZrO}_2$, and $\text{SrTi}_x\text{Zr}_{1-x}\text{O}_3$ Nanocrystal Photocatalysts with Bimetallic Pt-Ag Loading

By: Nicharee Chaona


Program: Petrochemical Technology

Thesis Advisors: Prof. Sumaeth Chavadej
Assoc. Prof. Pramoch Rangsunvigit


Accepted by the Petroleum and Petrochemical College, Chulalongkorn University, in partial fulfilment of the requirements for the Degree of Master of Science



..... College Dean
(Asst. Prof. Pomthong Malakul)

Thesis Committee:


.....
(Prof. Sumaeth Chavadej)


.....
(Assoc. Prof. Pramoch Rangsunvigit)


.....
(Assoc. Prof. Apanee Leungnaruemitchai)


.....
(Dr. Tarawipa Puangpetch)

ABSTRACT

5371012063: Petrochemical Technology Program
Nicharee Chaona: Hydrogen Production from Water Splitting under Visible Light Irradiation over Mesoporous-Assembled $\text{TiO}_2\text{-SiO}_2$, $\text{TiO}_2\text{-ZrO}_2$, and $\text{SrTi}_x\text{Zr}_{1-x}\text{O}_3$ Nanocrystal Photocatalysts with Bimetallic Pt-Ag Loading
Thesis Advisors: Prof. Sumaeth Chavadej and Assoc. Prof. Pramoch Rangsunvigit 110 pp.
Keywords: Photocatalysis/ Water splitting/ Hydrogen production/ Mesoporosity/ Bimetallic/ Visible light/

Hydrogen is an ideal energy source for the future due to its versatile application and environmentally friendly properties. Photocatalytic water splitting is a chemical reaction for producing hydrogen by using water and solar energy. This work focused on hydrogen production from photocatalytic water splitting under visible light irradiation using Eosin Y-sensitized mesoporous-assembled $\text{TiO}_2\text{-SiO}_2$, $\text{TiO}_2\text{-ZrO}_2$, and $\text{SrTi}_x\text{Zr}_{1-x}\text{O}_3$ photocatalysts with bimetallic Pt-Ag loading were synthesized by the sol-gel process with the aid of a structure-directing surfactant at the Ti-to-Si molar ratio of 97:3 calcined at 500 °C, Ti-to-Zr molar ratio of 93:7 calcined at 500 °C, and $\text{SrTi}_x\text{Zr}_{1-x}\text{O}_3$ with Ti-to-Zr molar ratio of 93:7 calcined at 700 °C. The photocatalytic activity, including phase composition, and Pt and Ag loadings, were investigated. The experimental results showed that the bimetallic Pt-Ag loadings with suitable contents by the photochemical deposition method were found to greatly enhance the photocatalytic activity of the assembled $0.97\text{TiO}_2\text{-}0.03\text{SiO}_2$, $0.93\text{TiO}_2\text{-}0.07\text{ZrO}_2$, and $\text{SrTi}_{0.93}\text{Zr}_{0.07}\text{O}_3$ photocatalyst.

บทคัดย่อ

ณิชารีย์ ชาวนา: การผลิตไฮโดรเจนจากการแตกโมเลกุลของน้ำภายใต้สภาวะที่มีแสงในช่วงตามองเห็นโดยใช้ตัวเร่งปฏิกิริยาไททาเนียมไดออกไซด์-ซิลิคอนไดออกไซด์, ไททาเนียมไดออกไซด์-เซอร์โคเนียมไดออกไซด์ และ สตรอนเทียมไททาเนียมเซอร์โคเนตที่เกาะตัวกันจนมีรูพรุนขนาดเมโซพอร์ที่ถูกกระตุ้นด้วยโลหะแบบผสมของแพลทินัมและซิลเวอร์ (Hydrogen Production from Water Splitting under Visible Light Irradiation over Mesoporous-Assembled $\text{TiO}_2\text{-SiO}_2$, $\text{TiO}_2\text{-ZrO}_2$, and $\text{SrTi}_x\text{Zr}_{1-x}\text{O}_3$ Nanocrystal Photocatalysts with Bimetallic Pt-Ag Loading) อ. ที่ปรึกษา : ศ. ดร. สุเมธ ชวเดช และ รศ. ดร. ปราโมช รังสรรค์วิจิตร 110 หน้า

ไฮโดรเจน เป็นแหล่งพลังงานในอนาคต เนื่องจาก ไฮโดรเจนมีประโยชน์หลายอย่างและเป็นมิตรกับสิ่งแวดล้อม ปฏิกิริยาการแตกโมเลกุลของน้ำโดยใช้ตัวเร่งปฏิกิริยาแบบใช้แสงร่วมเป็นกระบวนการในอนาคตในการผลิตไฮโดรเจน โดยการใช้แสงและพลังงานแสงงานวิจัยนี้มุ่งเน้นการผลิตไฮโดรเจนจากกระบวนการแตกโมเลกุลของน้ำด้วยปฏิกิริยาแบบใช้แสงร่วมภายใต้สภาวะที่มีแสงในช่วงที่ตามองเห็น โดยใช้ตัวเร่งปฏิกิริยาแบบใช้แสงร่วมไททาเนียมไดออกไซด์-ซิลิคอนไดออกไซด์, ไททาเนียมไดออกไซด์-เซอร์โคเนียมไดออกไซด์ และ สตรอนเทียมไททาเนียมเซอร์โคเนต ที่มีการเติมตัวเร่งปฏิกิริยาร่วมโลหะแบบผสมของแพลทินัมและเงิน โดยมีการกระตุ้นด้วยสีข้อม โดยตัวเร่งปฏิกิริยาแบบใช้แสงร่วมดังกล่าวถูกสังเคราะห์ขึ้นโดยกระบวนการโซลเจลควบคู่กับการใช้สารลดแรงตึงผิวเป็นสารต้นแบบ ที่มีอัตราส่วนโดยโมลของไททาเนียมไดออกไซด์ต่อซิลิคอนไดออกไซด์ที่ค่า 97 ต่อ 3 แคลไซน์ที่อุณหภูมิ 500 องศาเซลเซียส, ไททาเนียมไดออกไซด์ต่อเซอร์โคเนียมไดออกไซด์ที่ค่า 93 ต่อ 7 แคลไซน์ที่อุณหภูมิ 500 องศาเซลเซียส และสตรอนเทียมไททาเนียมเซอร์โคเนตที่มีอัตราส่วนโดยโมลของไททาเนียมไดออกไซด์ต่อเซอร์โคเนียมไดออกไซด์ที่ค่า 93 ต่อ 7 แคลไซน์ที่อุณหภูมิ 700 องศาเซลเซียส โดยได้ศึกษาถึงประสิทธิภาพในการเร่งปฏิกิริยาแบบใช้แสงร่วมของตัวเร่งปฏิกิริยาด้วยการเติมแพลทินัมและเงิน จากผลการทดลองพบว่าโลหะแบบผสมของแพลทินัมและเงิน ในปริมาณที่เหมาะสมบนพื้นผิวของตัวเร่งปฏิกิริยาแบบใช้แสงร่วมด้วยวิธีการยึดเกาะด้วยกระบวนการเคมีโดยใช้แสงร่วม ถูกพบว่าช่วยเพิ่มประสิทธิภาพการผลิตไฮโดรเจนของตัวเร่งปฏิกิริยาแบบใช้แสงร่วมไททาเนียมไดออกไซด์-ซิลิคอนไดออกไซด์, ไททาเนียมไดออกไซด์-เซอร์โคเนียมไดออกไซด์ และ สตรอนเทียมไททาเนียมเซอร์โคเนต อย่างมาก

ACKNOWLEDGEMENTS

This thesis work is funded by the Petroleum and Petrochemical College, and by the Center of Excellence on Petrochemical and Materials Technology, Thailand.

The author would like to express her sincere gratitude to Prof. Sumaeth Chavadej and Assoc.Prof. Pramoch Rungsunvigit for their invaluable guidance, understanding, and constant encouragement throughout the course of this research.

She would like to express special thanks to Assoc. Prof. Apanee Luengnaruemitchai and Dr. Tarawipa Puangpetch for kindly serving on her thesis committee. Their sincere suggestions are definitely imperative for accomplishing her thesis.

Her gratitude is absolutely extended to all staffs of the Petroleum and Petrochemical College, Chulalongkorn University, for all their kind assistance and cooperation.

Furthermore, she would like to take this important opportunity to thank all of her graduate friends for their unforgettable friendship.

Finally, she really would like to express her sincere gratitude to her parents and family for the love, understanding, and cheering.

TABLE OF CONTENTS

	PAGE
Title Page	i
Abstract (in English)	iii
Abstract (in Thai)	iv
Acknowledgements	v
Table of Contents	vi
List of Tables	ix
List of Figures	xi
 CHAPTER	
I INTRODUCTION	1
 II LITERATURE REVIEW	
2.1 Hydrogen: Fuel of the Future	3
2.2 Water Splitting: Hydrogen Generation Using Solar Energy	4
2.2.1 Photocatalytic Reaction	4
2.2.2 Splitting Water into Hydrogen	6
2.2.3 Efficiency	8
2.2.4 Semiconductor	8
2.2.5 Types of Semiconductor Systems Proposed for Solar Water Splitting	9
2.2.5.1 Semiconductor Solid State Photovoltaic Based Systems	9
2.2.5.2 Semiconductor Electrode (Liquid Junction) Systems	10
2.2.5.3 Semiconductor Particle Systems	11
2.2.6 The Principle of Water Splitting Using Semiconductor Particle	12
2.3 Photocatalyst	14

CHAPTER	PAGE
2.4 Titanium Oxide Photocatalyst	15
2.4.1 General Remarks	15
2.4.2 Crystal Structure and Properties	16
2.4.3 Semiconductor Characteristic and Photocatalytic Activity	18
2.5 Nano-Photocatalyst	20
2.5.1 General Remarks	20
2.5.2 Activity of Nano-Photocatalyst	21
2.6 Chemical Additive for Enhancement of Photocatalytic H ₂ Production	22
2.7 Metal Loading for Enhancement of H ₂ Production	24
2.8 Ion Doping for Enhancement of H ₂ Production	25
2.8.1 Metal Ion Doping	25
2.8.2 Anion Doping	27
2.9 Dye Sensitization	29
2.10 Composite Semiconductors	31
2.11 Mixed Oxide System	33
2.12 Bimetallic System	36
2.13 Porous Material	37
2.14 Sol-Gel Process	39
 III EXPERIMENTAL	 42
3.1 Materials and Equipment	42
3.1.1 Chemicals	42
3.1.2 Equipment	42
3.2 Experimental Procedures	43
3.2.1 Mesoporous-Assembled TiO ₂ -SiO ₂ Nanocrystal Photocatalyst Synthesis by a Sol-Gel Process with the Aid of a Structure-Directing Surfactant	43

CHAPTER	PAGE
3.2.2 Mesoporous-Assembled TiO ₂ -ZrO ₂ Nanocrystal Photocatalyst Synthesis by a Sol-Gel Process with the Aid of a Structure-Directing Surfactant	46
3.2.3 Mesoporous-Assembled SrTi _x Zr _{1-x} O ₃ Nanocrystal Photocatalyst Synthesis by a Sol-Gel Process with the Aid of a Structure-Directing Surfactant	49
3.2.4 Photocatalyst Characterizations	52
3.2.5 Photocatalytic H ₂ Production System	53
IV RESULTS AND DISCUSSION	55
4.1 Photocatalyst Characterizations	55
4.1.1 TG-DTA Results	55
4.1.2 N ₂ Adsorption-Desorption Results	60
4.1.3 XRD Results	68
4.1.4 UV-Visible Spectroscopy Results	75
4.1.5 SEM-EDX Results	84
4.1.6 TEM-EDX Results	89
4.1.7 Hydrogen Chemisorption Results	95
4.2 Photocatalytic Hydrogen Production Activity	96
4.2.1 Effect of Bimetallic Pt-Ag Loadings	97
V CONCLUSIONS AND RECOMMENDATIONS	101
5.1 Conclusions	101
5.2 Recommendations	101
REFERENCES	102
CURRICULUMVITAE	110

LIST OF TABLES

TABLE		PAGE
2.1	Definitions about porous solids	38
4.1	Thermal decomposition result of the dried synthesized pure TiO_2 , $0.97\text{TiO}_2\text{-}0.03\text{SiO}_2$, and $0.093\text{TiO}_2\text{-}0.07\text{ZrO}_2$ mixed oxide photocatalysts from TG-DTG analysis	58
4.2	Thermal decomposition result of the dried synthesized SrTiO_3 and $\text{SrTi}_{0.97}\text{Zr}_{0.03}\text{O}_3$ photocatalysts from TG-DTG analysis	60
4.3	N_2 adsorption-desorption results of the synthesized mesoporous-assembled pure TiO_2 , $0.97\text{TiO}_2\text{-}0.03\text{SiO}_2$, $0.93\text{TiO}_2\text{-}0.07\text{ZrO}_2$, SrTiO_3 and SrTiZrO_3 photocatalysts	66
4.4	N_2 adsorption-desorption results of the synthesized bimetallic Pt-Ag-loaded mesoporous-assembled $0.97\text{TiO}_2\text{-}0.03\text{SiO}_2$, $0.93\text{TiO}_2\text{-}0.07\text{ZrO}_2$, and $\text{SrTi}_{0.93}\text{Zr}_{0.07}\text{O}_3$ photocatalysts	67
4.5	Crystallite size results of the synthesized mesoporous-assembled pure TiO_2 , $0.97\text{TiO}_2\text{-}0.03\text{SiO}_2$, $0.93\text{TiO}_2\text{-}0.07\text{ZrO}_2$, pure SrTiO_3 and $\text{SrTi}_{0.93}\text{Zr}_{0.07}\text{O}_3$ photocatalysts	71
4.6	Crystallite size results of the synthesized bimetallic Pt-Ag-loaded mesoporous-assembled $0.97\text{TiO}_2\text{-}0.03\text{SiO}_2$, $0.93\text{TiO}_2\text{-}0.07\text{ZrO}_2$, and $\text{SrTi}_{0.93}\text{Zr}_{0.07}\text{O}_3$ photocatalysts calcined at $500\text{ }^\circ\text{C}$, $500\text{ }^\circ\text{C}$, and $700\text{ }^\circ\text{C}$, respectively	75

TABLE	PAGE
4.7 Absorption onset wavelength and band gap energy results of the synthesized mesoporous-assembled $0.97\text{TiO}_2\text{-}0.03\text{SiO}_2$, $0.93\text{TiO}_2\text{-}0.07\text{ZrO}_2$, and $\text{SrTi}_{0.93}\text{Zr}_{0.07}\text{O}_3$ photocatalysts	82
4.8 Absorption onset wavelength and band gap energy results of the synthesized mesoporous-assembled $0.97\text{TiO}_2\text{-}0.03\text{SiO}_2$, $0.93\text{TiO}_2\text{-}0.07\text{ZrO}_2$, and $\text{SrTi}_{0.93}\text{Zr}_{0.07}\text{O}_3$ photocatalysts with bimetallic Pt-Ag loadings	83
4.9 Metal dispersion results over the bimetallic Pt-Ag-loaded mesoporous-assembled $0.97\text{TiO}_2\text{-}0.03\text{SiO}_2$, $0.93\text{TiO}_2\text{-}0.07\text{ZrO}_2$, and $\text{SrTi}_{0.93}\text{Zr}_{0.07}\text{O}_3$ photocatalysts calcined at 500 °C, 500 °C, and 700 °C, respectively	96

LIST OF FIGURES

FIGURE	PAGE	
2.1	Relative emissions of greenhouse gases (expressed in carbon units per km) for vehicles powered by today's internal combustion engine using gasoline compared to vehicles powered by fuel cells	4
2.2	Types of photocatalytic reactions: (a) photoinduced reaction and (b) photon energy conversion reaction	5
2.3	Electrochemical cell in which the TiO ₂ electrode is connected with a Pt electrode	7
2.4	The structure of band gap energy	9
2.5	Schematic of (a) solid state photovoltaic cell driving a water electrolyzer and (b) cell with immersed semiconductor p/n junction (or metal/semiconductor Schottky junction) as one electrode	10
2.6	Schematic of liquid junction semiconductor electrode cell	11
2.7	Representation of semiconductor particulate system for heterogeneous Photocatalysis	12
2.8	Reaction schematic for water spitting reaction over semiconductor photocatalysts	13
2.9	Processes occurring in semiconductor photocatalyst under photoexcitation for water splitting reaction	14
2.10	Band gap energy of the photocatalyst	15
2.11	Crystal structures of (a) anatase, (b) rutile, and (c) brookite	16
2.12	Photocatalytic hydrogen production over anatase/rutile TiO ₂ under the mediation of I ⁻ /IO ₃ ⁻	23
2.13	Mechanism of dye-sensitized photocatalytic hydrogen production under visible light irradiation	30
2.14	Electron injection in composite semiconductors	32

FIGURE	PAGE
2.15 Proposed mechanism of phenol degradation at the surface of Ag/Au-TiO ₂ nanoparticles	37
2.16 A schematic of forming the BaTiO ₃ nanoparticles	40
3.1 Synthesis procedure for mesoporous-assembled 0.97TiO ₂ -0.03SiO ₂ photocatalysts: (a) without and (b) with Pt and/or Ag-loading by PCD method	45
3.2 Synthesis procedure for mesoporous-assembled 0.93TiO ₂ -0.07ZrO ₂ photocatalysts: (a) without and (b) with Pt and/or Ag-loading by PCD method	48
3.3 Synthesis procedure for mesoporous-assembled SrTiZrO ₃ photocatalysts: (a) without and (b) with Pt and/or Ag-loading by PCD method	51
3.4 Setup of photocatalytic H ₂ production system	54
4.1 TG-DTA curves of the dried synthesized (a) pure TiO ₂ , (b) 0.97TiO ₂ -0.03SiO ₂ , and (c) 0.93TiO ₂ -0.07ZrO ₂ photocatalysts	57
4.2 TG-DTA curves of the dried synthesized (a) SrTiO ₃ and (b) SrTi _{0.93} Zr _{0.07} O ₃ photocatalysts	59
4.3 N ₂ adsorption-desorption isotherms and pore size distributions (inset) of the synthesized mesoporous-assembled photocatalysts calcined at 500 °C: (a) pure TiO ₂ , (b) 0.97TiO ₂ -0.03SiO ₂ and (c) 0.93TiO ₂ -0.07ZrO ₂	63
4.4 N ₂ adsorption-desorption isotherms and pore size distribution (inset) of the synthesized 1.25 wt.% Pt-0.25 wt.% Ag-loaded mesoporous-assembled 0.97TiO ₂ -0.03SiO ₂ photocatalyst calcined at 500 °C	63

FIGURE	PAGE
4.5 N_2 adsorption-desorption isotherms and pore size distribution (inset) of the synthesized 0.25 wt.% Pt-1.25 wt.% Ag-loaded mesoporous-assembled $0.93TiO_2-0.07ZrO_2$ photocatalysts calcined at 500 °C	64
4.6 N_2 adsorption-desorption isotherms and pore size distributions (inset) of the synthesized mesoporous-assembled photocatalysts calcined at 700 °C: (a) $SrTiO_3$ and (b) $SrTi_{0.93}Zr_{0.07}O_3$	65
4.7 N_2 adsorption-desorption isotherms and pore size distribution (inset) of the synthesized 1.25 wt.% Pt-0.25 wt.% Ag-loaded mesoporous-assembled $SrTi_{0.93}Zr_{0.07}O_3$ photocatalysts calcined at 500 °C	65
4.8 XRD patterns of the synthesized mesoporous-assembled pure TiO_2 , $0.97TiO_2-0.03SiO_2$, and $0.93TiO_2-0.07ZrO_2$ photocatalysts calcined at 500 °C, (A = Anatase TiO_2).	69
4.9 XRD patterns of the synthesized mesoporous-assembled pure $SrTiO_3$ and $SrTi_{0.93}Zr_{0.07}O_3$ photocatalysts calcined at 700 °C	70
4.10 XRD patterns of the synthesized bimetallic Pt-Ag-loaded mesoporous-assembled $0.97TiO_2-0.03SiO_2$ photocatalysts calcined at 500 °C, (A = Anatase TiO_2)	72
4.11 XRD patterns of the synthesized bimetallic Pt-Ag-loaded mesoporous-assembled $0.93TiO_2-0.07ZrO_2$ photocatalysts calcined at 500 °C (A = Anatase TiO_2)	73
4.12 XRD patterns of the synthesized bimetallic Pt-Ag-loaded mesoporous-assembled $SrTi_{0.93}Zr_{0.07}O_3$ photocatalysts calcined at 700 °C	74

FIGURE	PAGE
4.13 UV-visible spectra of the synthesized mesoporous-assembled photocatalysts calcined at 500 °C: (a) pure TiO ₂ , and (b) 0.97TiO ₂ -0.03SiO ₂ , and (c) 0.93TiO ₂ -0.07ZrO ₂	77
4.14 UV-visible spectra of the synthesized mesoporous-Assembled photocatalysts calcined at 700 °C: (a) SrTiO ₃ and (b) SrTi _{0.93} Zr _{0.07} O ₃	78
4.15 UV-visible spectra of the synthesized mesoporous-assembled photocatalysts calcined at 500 °C: (a) 0.97TiO ₂ -0.03SiO ₂ and (b) 1.25 wt.% Pt-0.25 wt.% Ag-loaded 0.97TiO ₂ -0.03SiO ₂	79
4.16 UV-visible spectra of the synthesized mesoporous-assembled photocatalysts calcined at 500 °C: (a) 0.93TiO ₂ -0.07ZrO ₂ and (b) 0.25 wt.% Pt-1.25 wt.% Ag-loaded 0.93TiO ₂ -0.07ZrO ₂	80
4.17 UV-visible spectra of the synthesized mesoporous-assembled photocatalysts calcined at 700 °C: (a) SrTi _{0.93} Zr _{0.07} O ₃ and (b) 1.25 wt.% Pt-0.25 wt.% Ag-loaded SrTi _{0.93} Zr _{0.07} O ₃	81
4.18 UV-visible spectrum of Eosin Y solution	81
4.19 SEM images of the synthesized mesoporous-assembled photocatalysts calcined at 500 °C: (a) 0.97TiO ₂ -0.03SiO ₂ and (b) 1.25 wt.% Pt-0.25 wt.% Ag-loaded 0.97TiO ₂ -0.03SiO ₂	84
4.20 SEM images of the synthesized mesoporous-assembled photocatalysts calcined at 500 °C: (a) 0.93TiO ₂ -0.07ZrO ₂ and (b) 0.25 wt.% Pt-1.25 wt.% Ag-loaded 0.93TiO ₂ -0.07ZrO ₂	85

FIGURE	PAGE
4.21 SEM images of the synthesized mesoporous-assembled photocatalysts calcined at 700 °C: (a) $\text{SrTi}_{0.93}\text{Zr}_{0.07}\text{O}_3$ and (b) 1.25 wt.% Pt-0.25 wt.% Ag-loaded $\text{SrTi}_{0.93}\text{Zr}_{0.07}\text{O}_3$	85
4.22 SEM image and EDX area mappings of the synthesized 1.25 wt.% Pt-0.25 wt.% Ag-loaded mesoporous-assembled $0.97\text{TiO}_2\text{-}0.03\text{SiO}_2$ photocatalysts calcined at 500 °C	86
4.23 SEM image and EDX area mappings of the synthesized 1.25 wt.% Pt-0.25 wt.% Ag-loaded mesoporous-assembled $0.93\text{TiO}_2\text{-}0.07\text{ZrO}_2$ photocatalysts calcined at 500 °C	87
4.24 SEM image and EDX area mappings of the synthesized 1.25 wt.% Pt-0.25 wt.% Ag-loaded mesoporous-assembled $\text{SrTi}_{0.93}\text{Zr}_{0.07}\text{O}_3$ photocatalysts calcined at 700 °C	88
4.25 TEM images of synthesized mesoporous-assembled photocatalysts calcined at 500 °C: (a) pure TiO_2 , (b) $0.97\text{TiO}_2\text{-}0.03\text{SiO}_2$, and (c) $0.93\text{TiO}_2\text{-}0.07\text{ZrO}_2$	90
4.26 TEM images of synthesized mesoporous-assembled photocatalysts calcined at 700 °C: (a) pure SrTiO_3 and (b) $\text{SrTi}_{0.93}\text{Zr}_{0.07}\text{O}_3$	91
4.27 TEM image and EDX point mapping of the synthesized 1.25 wt.% Pt-0.25 wt.% Ag-loaded mesoporous-assembled $0.97\text{TiO}_2\text{-}0.03\text{SiO}_2$ photocatalyst calcined at 500 °C	92
4.28 TEM image and EDX point mapping of the synthesized 1.25 wt.% Pt-1.25 wt.% Ag-loaded mesoporous-assembled $0.93\text{TiO}_2\text{-}0.07\text{ZrO}_2$ photocatalyst calcined at 500 °C	93

FIGURE	PAGE	
4.29	TEM image and EDX point mapping of the synthesized 1.25 wt.% Pt-0.25 wt.% Ag-loaded mesoporous-assembled $\text{SrTi}_{0.93}\text{Zr}_{0.07}\text{O}_3$ photocatalyst calcined at 700 °C	94
4.30	Effect of bimetallic Pt-Ag loading on specific H_2 production rate over the mesoporous-assembled 0.97TiO_2 - 0.03SiO_2 photocatalyst calcined at 500 °C (Photocatalyst, 0.2 g; total reaction mixture volume, 150 ml; DEA concentration, 15 vol.%; E.Y. concentration, 0.1 mM; irradiation time, 5 h)	98
4.31	Effect of bimetallic Pt-Ag loading on specific H_2 production rate over the mesoporous-assembled 0.93TiO_2 - 0.07ZrO_2 photocatalyst calcined at 500 °C (Photocatalyst, 0.2 g; total reaction mixture volume, 150 ml; DEA concentration, 15 vol.%; E.Y. concentration, 0.1 mM; irradiation time, 5 h)	99
4.32	Effect of bimetallic Pt-Ag loading on specific H_2 production rate over the mesoporous-assembled $\text{SrTi}_{0.93}\text{Zr}_{0.07}\text{O}_3$ photocatalyst calcined at 700 °C (Photocatalyst, 0.2 g; total reaction mixture volume, 150 ml; DEA concentration, 15 vol.%; E.Y. concentration, 0.1 mM; irradiation time, 5 h)	100